# Mesomorphism in Segmented-Chain Polymers Containing Flexible Substituents in the Rigid Moiety

**Ugo Caruso, Stefania Pragliola, Antonio Roviello, and Augusto Sirigu***

*Dipartimento di Chimica, Università Federico II di Napoli, Via Mezzocannone 4, 80134 Napoli, Italy*

**Pio Iannelli**

*Dipartimento di Ingegneria Chimica ed Alimentare, Università di Salerno, Via Ponte Don Melillo, 84084 Fisciano (Sa), Italy*

*Received March 14, 1995; Revised Manuscript Received June 13, 1995*®

ABSTRACT: The synthesis and the phase behavior of a set of polymers characterized by having moderate chain flexibility and highly flexible lateral substituents are reported. The polymers have general formula $(-p\text{-}C_6H_4-OOC-p\text{-}C_6H_3(R)-COO-p\text{-}C_6H_4-O(CH_2)_nO-)_x$, with $R = -O(CH_2)_{m-1}CH_3$ ($m = 5-8$) and $n = 2, 4$. The presence of the lateral substituents, together with some chain flexibility, leads to comparatively low melting temperatures (lower than ~190 °C, for annealed samples) allowing a nematic liquid-crystalline behavior to show up in a thermotropic, enantiotropic way. X-ray diffraction data collected for annealed fibrous samples at room temperature indicate that the structural periodicity along the fiber axis substantially corresponds to the length of the monomer unit in its most extended conformation. The same holds for fibers not annealed. In this case, however, the regularity of the chain packing both along and across the fiber axis is drastically disturbed such that the solid state should better be classified as a mesophase.

## Introduction

Attaching lateral substituents of variable structure and bulkiness to the polymer chain of "main-chain" liquid-crystalline polymers may be done with very different purposes such as that of inducing chirality to obtain a cholesteric structure[1] or to introduce functional groups which allow cross-linking.[2,3] In most cases however, substitution is a practical means to influence basic properties such as solubility or melting and isotropization temperatures. For rigid-rod, fully aromatic polymers it is one of the few ways to obtain tractable materials with enantiotropic liquid-crystalline properties. Because of that, most of the main-chain liquid-crystalline polymers, containing lateral substituents consisting of flexible segments with no intrinsic mesogenic property, that have been studied have a rigid-rod type backbone.

Actually, flexible substituents have proven to be very effective in regulating polymer solubility and melting behavior, but frequently they have a deeper influence on the nature of mesomorphism itself changing the structure of the liquid-crystalline phase or giving rise to new structures.[4-12]

Concerning mesogenic polymers with segmented chains, no systematic examination is available of the influence exerted on the liquid-crystalline properties and on the solid-phase structure by the presence of flexible substituents at the rigid moiety. In the frame of our interest on liquid crystals derived from segmented-chain mesogenic polymers, we describe in this article the synthesis and a partial characterization of the liquid-crystalline and structural features of eight polymers with the formula

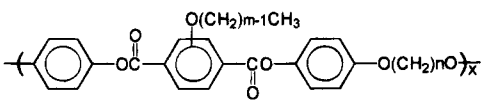


**P(n,m)** ; n = 2,4; m = 5,6,7,8

Polymers **P**($n$) corresponding to the unsubstituted backbone chain of **P**($n,m$) have already been reported[13,14] for $n = 5-10$. They are nematogenic, with melting temperatures ranging between ~230 and ~270 °C. As normally found for segmented-chain polymers, isotropization temperatures $T_i$ increase with decreasing length of the flexible spacer (e.g., $T_i = 351$ °C for $n = 6$)[14] with a steep gradient for low values of $n$. For polymers **P**(2) and **P**(4), corresponding to the backbone chains of **P**(2,$m$) and **P**(4,$m$), considerably higher values of both melting and isotropization temperatures should be expected, probably too high to be experimentally observable.

## Experimental Section

Polymers were synthesized by the condensation reaction of the appropriate couple of substituted terephthalic acid chloride and 4,4′-dihydroxy-1,$n$-diphenoxyalkane. An interfacial procedure was followed for polymers **P**(4,$m$) utilizing their fair solubility in chloroform at room temperature while polymers **P**(2,$m$) were obtained in $o$-dichlorobenzene solution at 180 °C.

**Synthesis of Precursors.** Substituted terephthalic acids were prepared starting from hydroxyterephthalic acid (referred to as compound **1**), whose synthesis was performed as follows: 20 g of aminoterephthalic acid is dissolved in 400 mL of cold 96% sulfuric acid. Keeping the solution at 5 °C and under stirring, 250 mL of cold 96% sulfuric acid containing freshly dissolved 15.2 g of sodium nitrite is added. After 2 h of reaction, 1 L of water is added; the solution is brought to boiling and kept for 3 h in such condition. Finally, 2 L of water are added, and the solution is left at room temperature overnight. The solid phase is then separated, washed several times with water, and dried in a vacuum at 110 °C (yield 80%). The compound melts at 320 °C with sublimation in accordance with the literature data.[15] The $^1$H NMR spectrum is in accordance with the formula.

2-(Alkoxy)terephthalic acids **2**($m$) were prepared by reaction of **1** and a large excess of the appropriate 1-bromoalkane in refluxing $N,N$-dimethylformamide in the presence of potassium carbonate. After 24 h, water was added and the organic phase extracted with chloroform. The chloroform solution was washed twice with water, and after a treatment with active carbon it was dried with sodium sulfate. The solvent was evaporated, and the residual oily phase dissolved in 95% ethanol and KOH added. **2**($m$) precipitates after a successive addition of water and acidification with HCl. A first purifica-

® Abstract published in *Advance ACS Abstracts,* August 1, 1995.

0024-9297/95/2228-6089$09.00/0 

**Table 1. Thermodynamic Data Concerning Substituted Terephthalic Acids 2(*m*) and Diphenols 3(*n*)[a]**

| 2(*m*); 3(*n*) | $T_{c-c}$ | $T_m$ | $\Delta H_m$ |
|---|---|---|---|
| 2(5) | 195 | 223 | 34.0 |
| 2(6) | 168 | 219 | 33.1 |
| 2(7) | 136 | 215 | 28.8 |
| 2(8) | 150 | 213 | 30.7 |
| 3(2) | | 227 | 63.4 |
| 3(4) | 202[b] | 207 | 60.8 |

[a] $T_{c-c}$/°C, solid-state transition temperature; $T_m$/°C, melting temperature. Temperatures are taken at the maximum of the relative DSC endotherm. $\Delta H_m$/kJ mol$^{-1}$, melting enthalpy. [b] 7.0 kJ mol$^{-1}$ transition enthalpy.

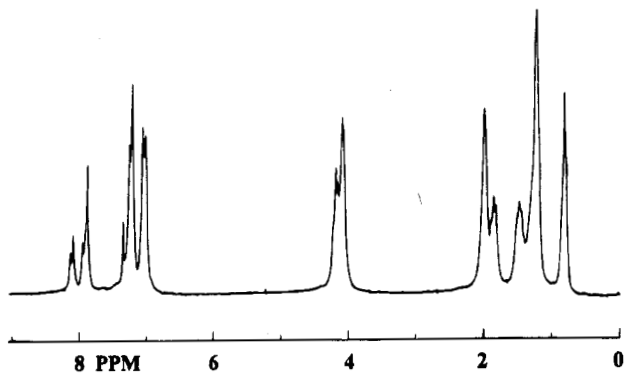


**Figure 1.** Polymer **P**(4,7). 200 MHz $^1$H NMR spectrum. $CDCl_3$ solution, 25 °C.

tion was obtained by a second precipitation from alkaline water solution and successive drying under vacuum. The acids thus obtained were further purified by transforming them into the corresponding chlorides and successive vacuum distillation (160 °C, 0.2 mmHg). Hydrolysis in ethanol–water–KOH solution and successive acidification with HCl produces **2**(*m*) (yield 50%). Melting temperatures and molar melting enthalpies are reported in Table 1. Contrary to what could be expected, melting enthalpies (and entropies as well) exhibit a decreasing trend with increasing *m*. This might be indicative of some disorder affecting the crystal structure. $^1$H NMR data are consistent with the expected formula for all compounds. $^{13}$C and $^1$H NMR data are specifically reported for compound **2**(7) taken as an example:

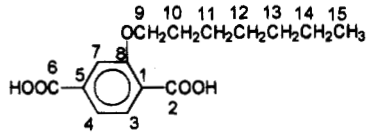


$^1$H NMR [δ (ppm), multiplicity] 3, 4 (7.67, m); 7 (7.70, d); 9 (4.13, m); 10 (1.84, m); 11–14 (1.36, m); 15 (0.91, m). $^{13}$C NMR (δ, ppm) 1, 4 (122.2, 122.0); 3, 5 (132.3, 132.4); 2, 6 (181.3); 7 (114.6); 8 (158.5); 9 (70.0); 10–14 (30.4, m); 15 (14.1).

Compounds HO–$C_6H_4$–*p*-O($CH_2$)$_n$O*p*–$C_6H_4$–OH (**3**(*n*), *n* = 2, 4) were prepared by reaction of the 1,*n*-dibromoalkanes with hydroquinone according to a procedure analogous to that already described by Griffin and Havens for the synthesis of homologues containing longer methylenic segments.[16] Both compounds are obtained as crystalline solids. The melting temperature of **3**(2) is 227 °C (222–224 °C reported by Kohn and Wilhelm[17]). **3**(4) melts at 207 °C (no literature data for comparison have been found). For both compounds, $^1$H NMR spectra are consistent with the expected formula.

**Polymer Synthesis.** Polymers **P**(2,*m*): equimolar amounts of the substituted terephthalic acid chloride and of the appropriate diphenol are dissolved in *o*-dichlorobenzene (previously treated under molecular sieves) in the ratio ~1 mmol/mL. The reaction proceeds 2 h at 180 °C under nitrogen atmosphere. After 2 h, 30 mL of boiling *o*-dichlorobenzene is added. The polymer is precipitated by addition of cold *n*-hexane, and after filtration, washed with *n*-hexane several times and oven dried at 110 °C for 3 h.

**Table 2. Solution Viscosity, Density, and Glass Transition Temperature[a]**

| polymer | [η] | ϱ | $T_g$ | polymer | [η] | ϱ | $T_g$ |
|---|---|---|---|---|---|---|---|
| **P**(2,5) | 0.807 | 1.209 | 90 | **P**(4,5) | 1.69[b] | 1.210 | 72 |
| **P**(2,6) | 0.485 | 1.209 | 86 | **P**(4,6) | 2.28 | 1.191 | 64 |
| **P**(2,7) | 0.504 | 1.221 | 77 | **P**(4,7) | 2.57 | 1.164 | 62 |
| **P**(2,8) | 0.505 | 1.212 | 73 | **P**(4,8) | 2.22 | 1.161 | 59 |

[a] Intrinsic viscosity, [η]/dL g$^{-1}$, measured at 120.0 °C in *o*-dichlorobenzene for **P**(2,*m*); at 25.0 °C in chloroform for **P**(4,*m*). Density/g cm$^{-3}$, measured at 25 °C on as extruded fibers; $\sigma(\varrho)/\varrho$ = 0.005. $T_g$/°C measured by DMTA methods. [b] 1.11 dL g$^{-1}$ at 120 °C in *o*-dichlorobenzene.

Polymers **P**(4,*m*): These polymers were all prepared by an interfacial reaction that we shall describe with some detail for **P**(4,5) only as an example. Pentanoxyterephthalic acid chloride (4.87 mmol) is dissolved in 40 mL of chloroform (previously treated under basic alumina) and the solution is added under vigorous stirring to a solution containing 4.92 mmol (1% stoichiometric excess) of diphenol **3**(4), 3.41 mmol of tetrabutylammonium hydrogen sulfate and 13.15 mmol of KOH in 90 mL of water. After 5 min, the polymer is precipitated by addition of 200 mL of *n*-hexane. Prolonged washing is sequentially operated with water (twice), chloroform/*n*-hexane 1/2 mixture (twice), ethanol, ethanol/water 1/1 mixture (twice), water (twice), ethanol. The polymer is dried for 2 h at 80 °C.

For all polymers synthesized the $^1$H NMR data are consistent with the formula. Figure 1 shows the $^1$H-NMR spectrum of **P**(4,7). Proton and $^{13}$C resonance data are specifically reported for polymer **P**(4,7) as an example:

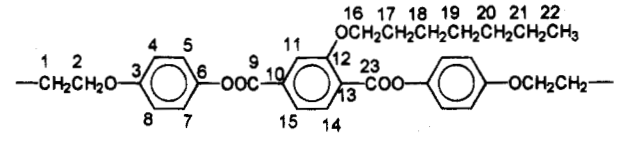


$^1$H NMR [δ (ppm), multiplicity 1 (1.40, m); 2 (4.07, t); 4, 8 (6.97, d); 5, 7 (7.17, d); 11 (8.00, d); 14, 15 (7.80, m); 16 (4.15, t); 17 (1.84, m); 18–21 (1.40, m); 22 (0.92, m). $^{13}$C NMR [δ (ppm)] 1 (31.6); 2 (67.8); 3 (156.8); 4, 8 (115.0); 5, 7 (122.4); 6 (144.1); 9, 23 (164.7); 10 (134.1); 11 (114.2); 12 (159.7); 13, 15 (121.4, d); 16 (69.2); 17–21 (25.9, m); 22 (14.0).

Utilizing an Ubbelohde viscometer, solution viscosity measurements were performed in *o*-dichlorobenzene at 120.00 ± 0.05 °C for polymers **P**(2,*m*) and in chloroform solution at 25.00 ± 0.02 °C for polymers **P**(4,*m*). Extrapolated intrinsic viscosities are reported in Table 2. The systematically higher values found for polymers **P**(4,*m*) are not to be ascribed entirely to the different measurement temperature. In fact, the intrinsic viscosity of polymer **P**(4,5) extrapolated from *o*-dichlorobenzene solution measurements at 120.00 ± 0.05 °C is [η] = 1.11 dL g$^{-1}$. This indicates that polymers obtained by interfacial synthesis have molecular weights higher than those obtained by solution polymerization.

Dynamic melt viscosity was measured at 10 Hz oscillation frequency utilizing a Rheometrics Recap II apparatus. Measurements were performed at decreasing temperature starting from the isotropic state.

Solid-state polymer densities (Table 2) were measured by flotation at 25 °C on as-extruded fibrous samples.

NMR spectra were recorded utilizing a Bruker 270 MHz and a Varian XL-200 spectrometer.

For X-ray diffraction data collection, the photographic technique was utilized. A cylindrical (57.3 mm radius) camera was used for room-temperature measurements with monochromatic Cr Kα (flat graphite single-crystal monochromator) radiation. For high-temperature measurements, a flat-film camera was employed (Ni-filtered Cu Kα radiation) equipped with a temperature-controlled microfurnace. Samples were closed under nitrogen atmosphere inside Lindemann capillaries.

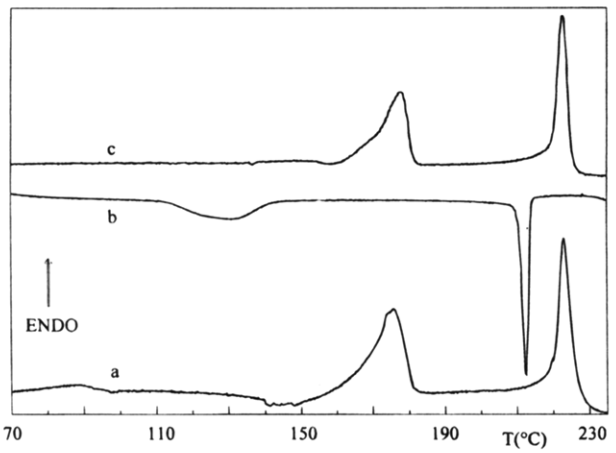


**Figure 2.** Polymer **P**(4,5). DSC behavior of a previously untreated sample. First heating run (curve a); first cooling run (curve b); second heating run (curve c).

**Table 3. Thermodynamic DSC Data Concerning Polymers**[a]

| polymer | $T_m$[b] | $\Delta H_m$[b] | $T_i$[b] | $\Delta H_i$[b] | $T_m$[c] | $\Delta H_m$[c] | $T_i$[c] | $\Delta H_i$[c] |
|---|---|---|---|---|---|---|---|---|
| **P**(2,5) | 168 | 7.0 | 235 | 9.8 | 173 | 9.9 | 232 | 10.1 |
| **P**(2,6) | 157 | 6.4 | 235 | 9.7 | 175 | 11.6 | 234 | 10.9 |
| **P**(2,7) | 176 | 9.5 | 228 | 9.1 | 185 | 11.7 | 231 | 9.2 |
| **P**(2,8) | 175 | 8.6 | 224 | 9.2 | 187 | 12.4 | 224 | 9.0 |
| **P**(4,5) | 177 | 8.9 | 222 | 10.0 | 180 | 12.5 | 222 | 10.3 |
| **P**(4,6) | 146 d | 6.1 | 220 | 10.0 | 153 | 8.9 | 218 | 10.1 |
| **P**(4,7) | 146 e | 6.4 | 214 | 9.8 | 153 | 9.6 | 213 | 9.5 |
| **P**(4,8) | 150 f | 5.5 | 213 | 8.3 | 153 | 10.6 | 210 | 9.6 |

[a] $T_m$/°C, melting temperature; $\Delta H_m$/J g$^{-1}$, melting enthalpy; $T_i$/°C, isotropization temperature; $\Delta H_i$/J g$^{-1}$, isotropization enthalpy. Temperatures are measured at the maximum of the transition endotherm. [b] Second DSC heating run from previously untreated samples. [c] Fibrous samples previously annealed for ~20 h at $T \sim T_m^c - 10$ °C. [d] Additional endothermic transition at 120 °C at the first heating run. [e] Additional endothermic transition at 130 °C at the first heating run. [f] Additional endothermic transition at 150 °C at the first heating run.

Phase transitions were examined by differential scanning calorimetry (Perkin-Elmer DSC-7 apparatus) at 10 °C/min temperature scanning rate under nitrogen atmosphere. Glass transition temperatures were measured by use of a PL DMTA apparatus at 10 Hz frequency and with a 5 °C/min temperature scanning rate.

For the optical observations a Zeiss polarizing microscope equipped with a Mettler microfurnace was used.

## Results and Discussion

Polarizing microscopy and DSC analysis show that all polymers **P**($n$,$m$) exhibit enantiotropic liquid-crystalline properties. The DSC behavior of a previously untreated sample of **P**(4,5) is reported in Figure 2 as an example. The isotropization corresponds to the endothermic transition peaked at 222 °C.

Table 3 reports for all polymers the thermodynamic data concerning the phase transitions measured for previously untreated samples and for annealed fibers. As expected, the annealing process increases melting temperatures and melting enthalpies as well. However, the latter quantities take in any case rather small values, quite comparable to isotropization enthalpies, and do not show any dependence on the length of the flexible substituent. This is true also for those polymers, namely, **P**(4,5) and all **P**(2,$m$) polymers, whose X-ray diffraction pattern is drastically changed with annealing and suggests that the flexible substituents might be conformationally rather disordered also in the crystalline state.

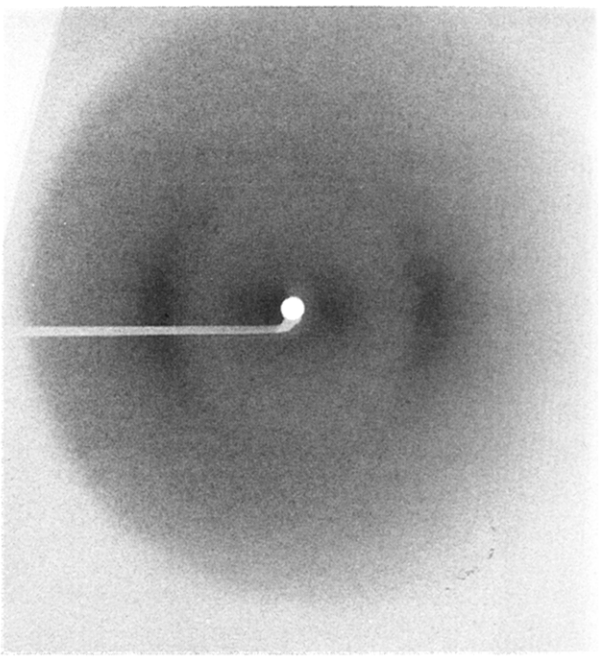

**Figure 3.** Polymer **P**(4,8). X-ray diffraction pattern recorded at 165 °C for a fibrous sample. The original macroscopic orientation is only partially maintained. Flat-film camera, Cu Kα.

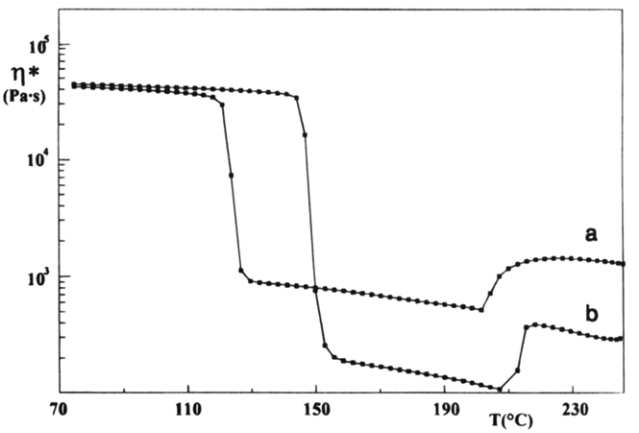


**Figure 4.** Dynamic viscosity curves for polymers **P**(4,8), curve a, and **P**(4,5), curve b.

Isotropization temperatures and enthalpies are substantially independent of the thermal treatment. Since the experimental error affecting the data is ~1% for temperatures and ~10% for enthalpies, differences to be observed in the data reported in Table 3 are of scarce statistical significance.

As to the nature of the liquid-crystalline phase, X-ray diffraction and dynamic viscosity measurements are consistent with a nematic structure. Figure 3 reports the X-ray diffraction pattern recorded at 165 °C for a fibrous sample of **P**(4,8) taken as an example. It is essentially characterized by an equatorial halo (the equatorial polarization simply indicates some persistence in the liquid phase of the original macroscopic orientation induced at the fiber extrusion) peaked at $\sin(\theta)/\lambda = 0.111$ Å$^{-1}$; no sharp Bragg diffraction is observable for lattice distances lower than ~41 Å. Further and more direct evidence in favor of the nematic nature of the liquid-crystalline phase is afforded by the dynamic viscosity measurement as a function of the temperature. Figure 4 shows the dynamic viscosity, measured at decreasing temperature starting from the isotropic

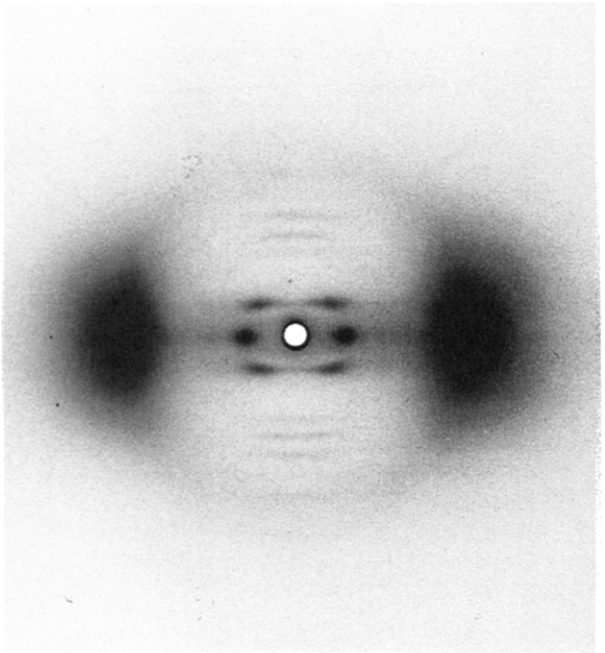

**Figure 5.** Polymer **P**(4,5). X-ray diffraction pattern of an as extruded fiber. Cylindrical camera, Cr Kα, room temperature.

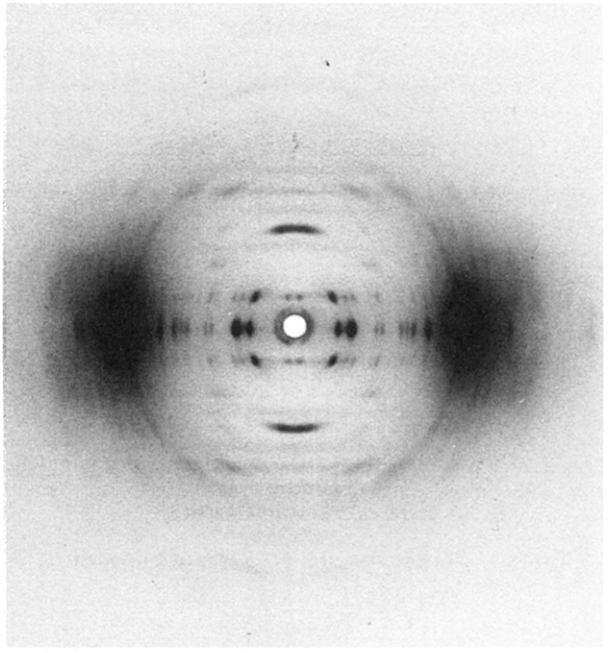

**Figure 6.** Polymer **P**(4,5). X-ray diffraction pattern of a fibrous sample previously annealed at 160 °C for 8 h. Cylindrical camera, Cr Kα, room temperature.

phase, for **P**(4,8) and **P**(4,5). In both cases, a sharp decrease of the melt viscosity marks the transition to the liquid-crystalline phase, as expected for nematics.

The thermal data reported in Table 3 indicate that (a) both for **P**(2,*m*) and **P**(4,*m*) isotropization temperatures are only moderately dependent on the length of the flexible substituent decreasing with increasing *m*; (b) polymers **P**(4,*m*) have lower isotropization temperatures than **P**(2,*m*) homologues; (c) isotropization enthalpies show small variations from the average value not immediately related to parameters *n* or *m*.

Features a and c are consistent with a role played by the flexible substituent as lateral groups having increasing bulkiness but substantially disordered structure. Feature b follows the trend, normally observed for segmented-chain polymers, which is related to an increased conformational flexibility as *n* increases.[18]

The presence of lateral substituents has a strong depressive influence on melting temperatures (Table 3). Actually, all polymers, even when a previous annealing has been operated, melt at temperatures which are drastically lower than the lowest one measured for unsubstituted analogues (229 °C for $n = 9$).[13] An analogous influence is apparently exerted on glass transition temperatures (Table 2), which decrease with increasing length of the substituent. Comparatively high values are found for polymers **P**(2,*m*) due to the higher conformational rigidity of the backbone chain. Annealing fibrous samples generally increases melting temperature and only modestly also melting enthalpy. This may be detected by comparison of the thermal data reported in Table 3. However, the X-ray diffraction analysis puts into light differences and similarities in the behavior of polymers **P**(2,*m*) and **P**(4,*m*).

For all polymers **P**(4,*m*), the X-ray diffraction pattern of as extruded fibers indicates poor crystallinity and very poor crystal perfection. The X-ray diffraction of **P**(4,5) is shown in Figure 5 as an example. It is essentially characterized by three intense diffractions. One of them, the most intense one, is a rather broad equatorial diffraction corresponding to a lattice distance of ~4.3 Å. The second intense equatorial diffraction corresponds to a lattice distance of 14.7 Å, while the third strong feature is a set of four correlated but not entirely resolved diffractions, corresponding to a lattice distance of 14.7 Å, whose ζ coordinates coincide with those of the *hk*1 layer line diffractions of the annealed fiber. No sharp modulated diffraction is observable along the other layer lines, only diffuse strips. In any case, a structural periodicity along the fiber axis of 22.9 Å is calculated from the *hk*1 layer line. This value is consistent with the length of the monomer unit in its extended conformation. Finally, it is worth noticing that a substantially equivalent diffraction pattern is obtained from not oriented samples, i.e., samples that have not been extruded in fibers.

The X-ray diffraction pattern of an annealed fiber of **P**(4,5) is reported in Figure 6. It indicates that although the same periodicity along the fiber axis is preserved some drastic structural change has occurred. It also shows that the diffraction pattern of the as-extruded fiber cannot be derived as a mere superimposition of diffractions from crystalline and noncrystalline (i.e., amorphous or liquid crystalline) fractions. On the other hand, the calorimetric behavior of the not annealed phase shows that melting does occur accompanied by a substantial enthalpic change. In conclusion, the phase whose X-ray diffraction is shown in Figure 5 should be considered as a mesophase distinguished both from the crystalline and liquid-crystalline phases.

The same conclusion should be drawn for the other **P**(4,*m*) polymers. Table 4 reports the relevant X-ray diffraction data for annealed and as extruded fibers. It must be noticed that while the periodicity along the fiber axis does not depend on *m* (as expected), the lattice distance of the strong equatorial diffraction at lower angle increases with increasing *m* as a consequence of the increasing bulk of the lateral substituent. At variance with the behavior of **P**(4,5), the crystallization of its homologues is scarcely influenced by annealing and the X-ray diffraction pattern of the annealed fiber indicates that a fraction of the polymer has still preserved the mesophase structure.

**Table 4. Measured Lattice Distances from Fibrous Samples[a]**

| | as extruded fibers | | | annealed fibers | | | |
|---|---|---|---|---|---|---|---|
| polymer | c | d(*hk0*) | d(*hkl*) | *T*(ann)[b] | *c* | *d*(*hk0*) | *d*(*hkl*) |
| **P**(2,5) | 20.6 | 16.4 vs<br>4.29 vs | 15.8 s | 160 | 20.6 | cryst[c] | |
| **P**(2,6) | 20.6 | 17.5 vs<br>10.5 vw<br>4.22 vs | 13.8 s<br>8.24 vw<br>3.40 w | 160 | 20.6 | cryst[c] | |
| **P**(2,7) | 20.6 | 18.4 vs<br>10.5 vw<br>6.94 vw<br>5.21 w<br>4.22 vs | 14.0 w<br>8.61 vw<br>3.40 vw | 170 | 20.6 | cryst[c] | |
| **P**(2,8) | 20.6 | 19.5 vs<br>11.0 vw<br>7.28 vw<br>5.19 w<br>4.22 vs | 14.0 w<br>8.66 vw<br>3.43 vw | 170 | 20.6 | cryst[c] | |
| **P**(4,5) | 22.9 | 14.7 vs<br>8.63 vw<br>4.37 vs | 14.7 s | 160 | 22.9 | cryst[c] | |
| **P**(4,6) | 22.9 | 16.4 vs<br>5.53 vw<br>4.33 vs | 15.7 s | 140 | 22.9 | 15.9 vs,<br>8.24 vw<br>8.58 vw<br>5.53 s<br>4.30 vs | 13.9 s |
| **P**(4,7) | 22.9 | 17.2 vs<br>5.45 w<br>4.31 vs | 16.2 s | 140 | 22.9 | 17.2 vs,<br>8.63 vw<br>5.49 s<br>4.32 vs | 14.2 s |
| **P**(4,8) | 22.9 | 18.0 vs<br>5.41 w<br>4.33 vs | 16.6 s | 140 | 22.9 | 17.8 vs,<br>5.40 w<br>4.32 vs<br>3.56 vw | 14.7 s |

[a] Lattice distances and crystallographic *c* axis in angstroms. Diffraction intensity on indicative visual basis. [b] *T*(ann)/°C, annealing temperature. [c] Extensively crystallized.

Table 4 reports also the lattice distances measured for polymers **P**(2,*m*). The data concern only as-extruded fibers. In fact, for this class of polymers, annealing (even if not particularly prolonged) has a large effect on crystallization. Some affinities with the data concerning polymers **P**(4,*m*), as well as some differences are apparent.

The periodicity along the fiber axis is 20.6 Å for all polymers and does not depend on the thermal treatment. This value is consistent with that measured for polymers **P**(4,*m*) and confirms the hypothesis that the backbone chain is in its most extended conformation for all polymers.

The lattice distance corresponding to the intense equatorial diffraction at lower angle increases with increasing length of the substituent and keeps for each *m* a higher value as compared to the **P**(4,*m*) homologue. This feature is not surprising on account of the larger value of the periodicity along the fiber axis measured for the latter, which allows packing the polymer chains with smaller average cross sections.

Figures 7 and 8 report the X-ray diffraction patterns of as-extruded and annealed fibrous samples of **P**(2,8), respectively. Several strong and sharp diffractions characterizing the pattern of the annealed fiber appear weakened and smeared or totally undetectable (e.g., the strong meridian 001 reflection) in the pattern of the unannealed one. Since analogous features are to be observed for all the other polymers, it may be concluded that as for polymers **P**(4,*m*), and notwithstanding the increased number of observed diffractions (at least for **P**(2,7) and **P**(2,8)) the not annealed phase of polymers **P**(2,*m*) is essentially a mesophase which cannot be dealt with in a straightforward way on the basis of the crystalline phase only.

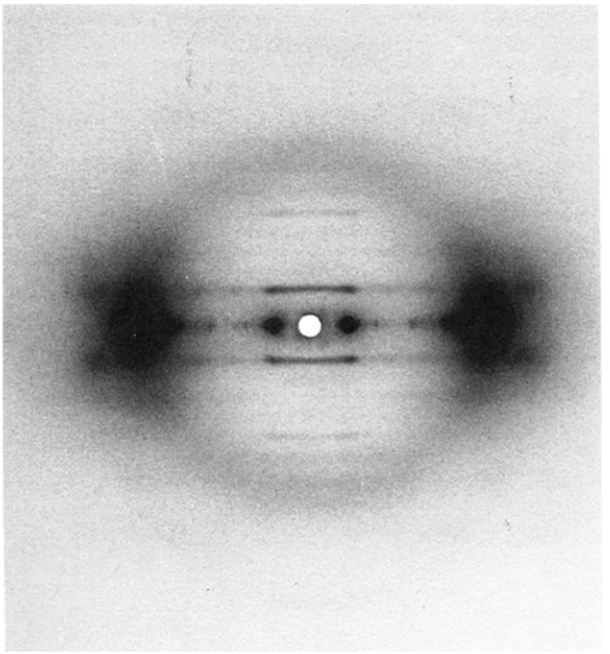

**Figure 7.** Polymer **P**(2,8). X-ray diffraction pattern of a an as extruded fiber. Cylindrical camera, Cr Kα, room temperature.

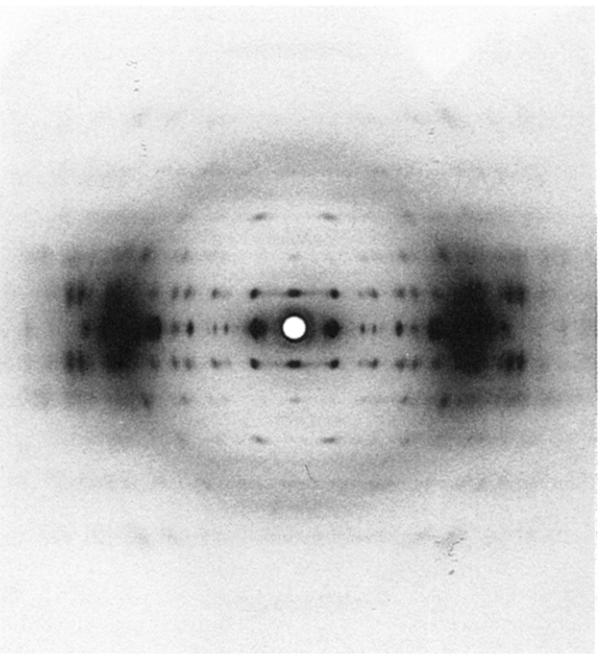

**Figure 8.** Polymer **P**(2,8). X-ray diffraction pattern of a fibrous sample previously annealed at 175 °C for 22 h. Cylindrical camera, Cr Kα, room temperature.

A more detailed examination of the crystalline phase has been made for polymer **P**(2,8). A possible unit cell has been calculated as a best fit to the experimentally measured lattice distances. Table 5 reports a comparison between experimental and calculated data for a hexagonal unit cell with the following parameters: $a = b = 21.22$ Å, $c = 20.86$ Å, $\alpha = \beta = 90°$, $\gamma = 120°$. For this unit cell, the best fit to the experimental density ($\varrho$(exp) = 1.205 ± 0.006 g cm$^{-3}$ at 25 °C; $\varrho$(calc) = 1.235 g cm$^{-3}$) is obtained with 12 monomer units/unit cell.

Notwithstanding the good agreement between calculated and experimental lattice distances reported in

**Table 5. Polymer P(2,8): Comparison between Calculated and Measured Lattice Distances for a Hexagonal Unit Cell with Lattice Parameters: $a = b = 21.22$ Å, $c = 20.86$ Å[a]**

| *hkl* | *d*(obs)/Å | *d*(calcd)/Å |
|---|---|---|
| 100,010,1$\bar{1}$0 | 18.38 vvs | 18.38 |
| 110, 2$\bar{1}$0, 1$\bar{2}$0 | 10.61 v | 10.61 |
| 200,020,2$\bar{2}$0 | 9.19 w | 9.19 |
| 210,120,3$\bar{1}$0,1$\bar{3}$0,3$\bar{2}$0,2$\bar{3}$0 | 6.98 s | 6.95 |
| 300,030,3$\bar{3}$0 | 6.11 w | 6.13 |
| 220,4$\bar{2}$0,2$\bar{4}$0 | 5.35 vs | 5.31 |
| 310,130,4$\bar{1}$0,1$\bar{4}$0,4$\bar{3}$0,3$\bar{4}$0 | 5.11 vs | 5.10 |
| 400,040,4$\bar{4}$0 | 4.57 vw | 4.60 |
| 320,230,5$\bar{2}$0,2$\bar{5}$0,5$\bar{3}$0,3$\bar{5}$0 | 4.23 vvs | 4.22 |
| 410,140,5$\bar{1}$0,1$\bar{5}$0,5$\bar{4}$0,4$\bar{5}$0 | 3.99 vs | 4.01 |
| 330,6$\bar{3}$0,3$\bar{6}$0 | 3.56 w | 3.54 |
| 240,420,6$\bar{2}$0,2$\bar{6}$0,6$\bar{4}$0,4$\bar{6}$0 | 3.48 w | 3.47 |
| 600,060,6$\bar{6}$0 | 3.06 vvw | 3.06 |
| 610,160 | 2.80 w | 2.80 |
| 101,011,1$\bar{1}$1 | 13.7 vs | 13.8 |
| 111,2$\bar{1}$1,1$\bar{2}$1 | 9.57 w | 9.46 |
| 201,021,2$\bar{2}$1 | 8.39 s | 8.41 |
| 211,121,1$\bar{3}$1,3$\bar{1}$1,3$\bar{2}$1,2$\bar{3}$1 | 6.54 s | 6.59 |
| 301,031,3$\bar{3}$1 | 5.89 s | 5.88 |
| 221,4$\bar{2}$1,2$\bar{4}$1 | 5.13 w | 5.14 |
| 311,131,4$\bar{1}$1,1$\bar{4}$1,3$\bar{4}$1,4$\bar{3}$1 | 5.00 w | 4.95 |
| 401,041,4$\bar{4}$1 | 4.48 vw | 4.49 |
| 321,231,5$\bar{2}$1,2$\bar{5}$1,5$\bar{3}$1,3$\bar{5}$1 | 4.12 s | 4.13 |
| 411,141,5$\bar{1}$1,1$\bar{5}$1,5$\bar{4}$1,4$\bar{5}$1 | 3.94 w | 3.94 |
| 501,051,5$\bar{5}$1 | 3.59 vw | 3.62 |
| 421,241,6$\bar{2}$1,2$\bar{6}$1,6$\bar{4}$1,4$\bar{6}$1 | 3.43 s | 3.43 |
| 511,151,6$\bar{1}$1,1$\bar{6}$1,6$\bar{5}$1,5$\bar{6}$1 | 3.26 s | 3.26 |
| 102,012,1$\bar{1}$2 | 9.10 vvw | 9.07 |
| 112,2$\bar{1}$2,1$\bar{2}$2 | 7.43 vw | 7.44 |
| 202,022,2$\bar{2}$2 | 6.82 vw | 6.90 |
| 212,122,3$\bar{1}$2,1$\bar{3}$2,3$\bar{2}$2,2$\bar{3}$2 | 5.66 s | 5.78 |
| 302,032,3$\bar{3}$2 | 5.29 w | 5.28 |
| 222,4$\bar{2}$2,2$\bar{4}$2 | 4.75 w | 4.73 |
| 312,132,4$\bar{1}$2,1$\bar{4}$2,4$\bar{3}$2,3$\bar{4}$2 | 4.51 s | 4.58 |
| 103,013,1$\bar{1}$3 | 6.49 s | 6.50 |
| 023,203,2$\bar{2}$3 | 5.59 w | 5.55 |
| 213,123,3$\bar{1}$3,1$\bar{3}$3,3$\bar{2}$3,2$\bar{3}$3 | 4.79 w | 4.91 |

[a] Observed intensities on an indicative visual basis. Possible *hkl* indexes corresponding to calculated lattice distances.

Table 5, the unit cell given should be taken as a first approach. Actually, at least two features suggest some caution. (i) The presence among the observed diffraction data of a very weak equatorial reflection with 8.36 Å lattice distance is not accounted for; this feature however, might also be indicative of the presence of a small amount of a second crystal form. (ii) The shape of the observed meridian diffraction corresponding to the 001 reflection (not reported in Table 5) suggests that the true unit cell might be not exactly hexagonal but slightly distorted toward a triclinic form. This conclusion is supported by the following feature. A progressive splitting of the same reflection is unmistakably observable in the diffraction pattern of the homologous polymers at decreasing length of the flexible substituent accompanied by a splitting of the very strong equatorial diffraction which has been indexed as 100 in the case of polymer **P**(2,8). All this indicates that the crystallographic *c* axis progressively deviates from the reciprocal *c** direction and that the packing across the chain axis progressively deviates from the hexagonal pattern.

**Acknowledgment.** Research supported by Ministero della Ricerca Scientifica e Tecnologica of Italy. The NMR spectra were recorded at the Centro di Metodologie Chimico-Fisiche of the University of Napoli. The authors are grateful to Prof. D. Acierno and Dr. M. Frigione of the University of Salerno for making dynamic viscosity measurements possible.

## References and Notes

(1) Fujishiro, K.; Lenz, R. W. *Macromolecules* **1992**, *25*, 81.
(2) Bualek, S.; Kapitza, H.; Meyer, J.; Schmidt, G. F.; Zentel, R. *Mol. Cryst. Liq. Cryst.* **1988**, *155*, 47.
(3) Caruso, U.; Pragliola, S.; Roviello, A.; Sirigu, A. *Macromolecules* **1993**, *26*, 221.
(4) Ballauff, M.; Schmidt, G. M. *Makromol. Chem., Rapid Commun.* **1987**, *8*, 93.
(5) Rodriguez-Parada, J. M.; Duran, R.; Wegner, G. *Macromolecules* **1989**, *22*, 2507.
(6) Kricheldorf, H. R.; Engelhardt, J. *Makromol. Chem.* **1990**, *191*, 2017.
(7) Stern, R.; Ballauff, M.; Lieser, G.; Wegner, G. *Polymer* **1991**, *32*, 2096.
(8) Lee, K. S.; Kim, H. M.; Rhee, J. M.; Lee, S. M. *Macromol. Chem.* **1991**, *192*, 1033.
(9) Harkness, B. R.; Watanabe, J. *Macromolecules* **1991**, *24*, 6759.
(10) Watanabe, J.; Harkness, B. R.; Sone, M. *Polym. J.* **1992**, *24*, 1119.
(11) Bao, Z.; Chen, Y.; Coi, R.; Yu, L. *Macromolecules* **1993**, *26*, 5281.
(12) Centore, R.; Roviello, A.; Sirigu, A.; Kricheldorf, H. R. *Macromol. Chem. Phys.* **1994**, *195*, 3009.
(13) Antoun, S.; Lenz, R. W.; Jin, J. I. *J. Polym. Sci., Polym. Chem. Ed.* **1981**, *19*, 1901.
(14) Uryu, T.; Kato, T. *Macromolecules* **1988**, *21*, 378.
(15) Morton, A. A.; Letsinger, R. L. *J. Am. Chem. Soc.* **1945**, *67*, 1537.
(16) Griffin, A. C.; Havens, S. J. *J. Polym. Sci., Polym. Phys. Ed.* **1981**, *19*, 951.
(17) Kohn, M.; Wihlelm, F. *Monatshefte f. Chem.* **1922**, *43*, 551.
(18) Sirigu, A. In *Liquid Crystallinity in Polymers*; Ciferri, A., Ed.; VCH Publishers: New York, 1991; Chapter 7.

MA950335E